Journal of Alloys and Compounds 619 (2015) 151–156

Contents lists available at ScienceDirect

Journal of Alloys and Compounds

journal homepage: www.elsevier.com/locate/jalcom

Near room temperature magneto-transport (TCR & MR) and magnetocaloric effect in $Pr_{2/3}Sr_{1/3}MnO_3$:Ag_2O composite

Ramesh Chandra Bhatt [a,b,*], V.P.S. Awana [a], H. Kishan [a], P.C. Srivastava [b]

[a] Quantum Phenomena and Applications Division, National Physical Laboratory (CSIR), New Delhi 110012, India
[b] Department of Physics, Banaras Hindu University, Varanasi 221005, India

ARTICLE INFO

Article history:
Received 2 July 2014
Received in revised form 6 August 2014
Accepted 25 August 2014
Available online 6 September 2014

Keywords:
Magnetic materials
Magnetocaloric effect
Refrigeration capacity

ABSTRACT

The magneto-transport and magnetocaloric effect in $Pr_{2/3}Sr_{1/3}MnO_3$:Ag_2O (PSMO:Ag) with Ag_2O (10–30 mol%) have been studied by resistivity and magnetization measurements. Temperature coefficient of resistance (TCR), magneto-resistance (MR) and magnetocaloric properties of the composite have shown different responses to Ag addition. Rietveld refinement confirms single phase crystalline structure with orthorhombic *Pbnm* space group and presence of silver metal as well. TCR changes randomly with Ag, increasing initially to 7.8% K^{-1} for PSMO:Ag10 composite which then decreases marginally with increasing Ag content. MR has been found to reach a maximum value of 30.5% at 1 T applied field for PSMO:Ag10 composite. Magnetic entropy change (ΔS_M) increases with increasing Ag content and is found to be 3.5 J kg^{-1} K^{-1} (1 T), 6.1 J kg^{-1} K^{-1} (2 T) and 8.4 J kg^{-1} K^{-1} (3 T) for PSMO:Ag30 composite at 285 K. The maximum refrigeration capacity of 39.5 J kg^{-1} (1 T), 91.0 J kg^{-1} (2 T) and 107.7 J kg^{-1} (3 T) has been found for the PSMO:Ag20 composite. PSMO:Ag composite exhibits potential for bolometric, magnetic sensing and magnetic refrigerating applications near room temperature.

1. Introduction

For years, colossal magneto-resistance (CMR) observed in perovskite manganites has attracted much attention to research into structural, magnetic, and electrical properties of these materials. Doping suitable amount of divalent alkaline earth in rare earth manganese oxides makes it ferromagnetic metal from the initially antiferromagnetic insulator, with accompanying metal to insulator transition and ferromagnetic–paramagnetic (FM–PM) phase transition at well-defined temperatures T_P and T_C respectively. Both magneto-resistance (MR) and temperature coefficient of resistance (TCR) exist around these temperatures (T_P and T_C). TCR is defined as $1/R \cdot (dR/dT)$, where R is the electrical resistance of the sample. A sharp *M–I* transition favors high TCR and materials with sharp TCR peak for a little temperature change have been demanding for room temperature bolometers. A high value of MR for low applied field is required for the magnetic sensing devices. More recently CMR manganites have also been the subject of research for their potential refrigerating capability at room temperature [1,2]. From application point of view one requires high value of magnetic entropy change (ΔS_M) for small change in magnetic field around room temperature which should also be constantly high over the entire temperature range [1,2]. Review article by Phan et al. shows a range of La-based manganites and a few Pr-based manganite near room temperature as active magnetic refrigerant materials (AMR) [1,3]. Further to enhance the TCR and MR, several Ag added La–manganite composites have been studied earlier [4–7]. The insulator oxide additive manganite composites have shown significant MR values but they shift the transition point towards the low temperature region relative to the pristine manganite with the similar behavior in the magnetocaloric effect (MCE). Only a few reports on MCE exist in metal–manganite composites. In the present communication we have chosen metal (Ag) oxide additive in Pr–manganite composite. We have also examined $Pr_{2/3}Sr_{1/3}MnO_3$:Ag_2O manganite composite for their magnetic refrigerating capability close to room temperature. Such a composite due to grain boundary effect is expected to exhibit significant TCR and MR properties close to room temperature.

2. Experimental

Polycrystalline composite samples of $(1-x)Pr_{2/3}Sr_{1/3}MnO_3 + (x)Ag_2O$ (x = 0, 10, 20 and 30 mol%) were synthesized by the standard solid-state reaction method. Powders of Pr_6O_{11}, $SrCO_3$ and MnO_2 were mixed in desired molar fractions. After proper mixing and grinding the mixture was calcined at 900 °C, 1000 °C and 1100 °C each for 24 h with intermediate grindings and the pellets were sintered

* Corresponding author at: Quantum Phenomena and Applications Division, National Physical Laboratory (CSIR), New Delhi 110012, India. Tel.: +91 11 45608276; fax: +91 11 45609310.
E-mail address: rcbhatt1986@gmail.com (R.C. Bhatt).

http://dx.doi.org/10.1016/j.jallcom.2014.08.216
0925-8388/

at 1350 °C for 24 h. Ag_2O is added in the as-prepared PSMO material and pelletized. The Ag_2O composites were finally sintered at 1350 °C for 1 $\frac{1}{2}$ h with furnace cooling to room temperature. Phase purity and the lattice parameter refining of the samples are checked through powder diffractometer using Cu Kα radiation (Rigaku) and the Rietveld refinement programme (Fullprof version). The grain size distribution and surface morphology are checked through scanning electron microscope (SEM). Elemental analysis is carried out using energy dispersive spectroscopy (EDS) attached with SEM. Electrical resistivity and magnetization measurements of the samples were carried out in magnetic field up to 3 T on a Physical Property Measurement System (Quantum Design, USA).

3. Results and discussion

Fig. 1 depicts the Rietveld refined X-ray diffraction patterns for the composite series $(1-x)Pr_{2/3}Sr_{1/3}MnO_3 + (x)Ag_2O$. All the samples are crystallized in orthorhombic perovskite structure with *Pbnm* space group. Rietveld analysis revealed that all the samples are phase pure except for the presence of metal Ag in the higher % of Ag_2O added composites (30%). The metal Ag peak is labelled as * in the diffraction pattern. The presence of metal Ag confirms the dissociation of Ag_2O into Ag during the sintering process due to its low dissociation temperature (350 °C). The lattice parameters have been listed in Table 1 and no considerable change in the unit cell parameters *a* (Å), *b* (Å), *c* (Å) and the cell volume (Å^3) is noticed with Ag addition.

The SEM micrographs of $(1-x)Pr_{2/3}Sr_{1/3}MnO_3 + (x)Ag_2O$ composites have been shown in Fig. 2. Fig. 2(a) depicts the grain morphology of the pristine PSMO material. The silver additive effect is clearly noticed in the micrographs of the composite material through shining regions around the PSMO grains (Fig. 2(b–d)).

The temperature dependence of electrical resistivity for the composite series has been shown in Fig. 3. The insulator–metal transition temperature T_P for PSMO:Ag10 and PSMO:Ag30 samples has been found to be around 300 K, however T_P for PSMO:Ag20 sample could not be ascertained as its the resistivity is seen to be increasing. Transition becomes sharper in Ag composites compared to pristine PSMO. Peak value of the electrical resistivity decreased from ~130 m Ω cm for PSMO to 21.5 m Ω cm for PSMO:Ag10 and ~4 m Ω cm for PSMO:Ag20 sample. The PSMO:Ag30 sample has the resistivity peak value of 14.6 m Ω cm. The composite PSMO:Ag20 has exhibited lower resistivity than PSMO:Ag30. The reason is the maximum limit on the amount of Ag that can be added to the grain boundaries (GB) of PSMO manganite. In the present case, it appears that this limit is between 20% and 30% Ag_2O addition. In this range extra silver may go to interstitial sites leading to an increase in the resistivity. The transmission electron microscopy (TEM) and electron energy loss spectroscopy (EELS) experiments [8] have shown that Ag cannot be substituted at the rare-earth site. Moreover, Ag cannot go to the Mn-sites also, as there is a large difference between the ionic size of Ag (*I.R.VI* = 1.15 Å) and the Mn ion (Mn^{3+}, *I.R.VI* = 0.645 Å; Mn^{4+}, *I.R.VI* = 0.53 Å) [9], Hume-Rothery criteria for ion substitution is also not satisfied. This proves the extra Ag going to the interstitials and the observed enhancement in the electrical resistivity (Fig. 3). The observed reduced resistivity in the Ag composites is due to the fact that the oxygen liberated from the Ag–O bond fills the vacancy in the Mn^{3+}–Mn^{4+} bond required for the electron transfer through double exchange phenomena. The temperature coefficient of resistance (TCR) of all the samples has been shown in the inset of Fig. 3. Since all the TCR values are close to temperature 282 K, therefore the data have been shifted by 4 K successively towards positive temperature axis to avoid the overlapping of the peaks. TCR of 2.3% K^{-1} for the PSMO sample has been enhanced to the maximum value of 7.8% K^{-1} for the PSMO:Ag10 composite which marginally decreased thereafter to 7.2 and 6.9% K^{-1} for PSMO:Ag20 and PSMO:Ag30 composites respectively.

Fig. 4 shows the temperature dependence of magneto-resistance for the pristine and Ag added PSMO composites at 1 T applied field in the perpendicular direction. Since the maximum MR values for all the samples have been found to be close to 284 K, the MR data have been intentionally shifted by 10 K successively towards the positive temperature axis for clear depiction. It has been noticed that the low temperature MR in PSMO has suppressed to negligibly small values for Ag composites. The reasons behind this are: (i) grain boundaries are non-conducting in PSMO (due to disorder, strain and spin scattering) which offer resistance to the conducting electrons. When field is applied the spins gets aligned in the field direction and hopping of electrons takes place which generates more MR, (ii) metallic Ag which is not going to the lattice sites is occupied in the grain boundaries and grain surfaces of PSMO therefore offers less resistance (or repairs disorder, strain and spin scattering) as compared to pristine PSMO and less MR is generated with the application of field. The near room temperature MR has been found to increase from 17% for PSMO to the maximum value of 30.5% for PSMO:Ag10 composite. For PSMO:Ag20 and PSMO:Ag30 composites the MR dropped only marginally to ~29%. Researchers usually have reported the maximum MR value in 27% Ag added manganite and less thereafter which was not in the present case [10]. The TCR and MR values in the present study have been found to be comparable or greater than some of the reported values in the literature viz. ~30% MR at 1 T with ~9% TCR (300 K) in $La_{0.7}Ca_{0.2}Sr_{0.1}MnO_3$:Ag [4], 25.5% MR at 1.2 T (310 K) in $La_{0.7}Ag_{0.3}MnO_3$ [11], ~24%, 34% MR at 1 T, 2 T respectively with 6.4% K^{-1} TCR (310 K) in $(La_{0.7}Ca_{0.2}Sr_{0.1}MnO_3)_{0.9}Pd_{0.1}$ [12], 23% at 5 T (300 K) in $(La_{0.7}Ca_{0.3}MnO_3)_{0.9}Ag_{0.1}$ [13], 31% MR at 1 T (300 K) in $La_{0.7}Ca_{0.2}Sr_{0.1}MnO_3$:Ag [5], 27% room temperature MR at 1.15 T in $La_{0.8333}Na_{0.167}MnO_3$:Ag [14], 40% room temperature MR at 2.5 T in $(La_{0.7}Ca_{0.2}Sr_{0.1}MnO_3)_{0.75}Ag_{0.25}$ [15], 25% room temperature MR at

Table 1
Rietveld refined lattice parameters and unit cell volume of the composite series $(1-x)Pr_{2/3}Sr_{1/3}MnO_3 + (x)Ag_2O$.

Sample	*a* (Å)	*b* (Å)	*c* (Å)	Vol. (Å^3)
PSMO	5.485 (9)	5.455 (4)	7.709 (9)	230.747
PSMO:Ag10	5.487 (0)	5.455 (7)	7.710 (2)	230.813
PSMO:Ag20	5.487 (7)	5.457 (0)	7.710 (7)	230.909
PSMO:Ag30	5.486 (7)	5.455 (9)	7.710 (3)	230.810

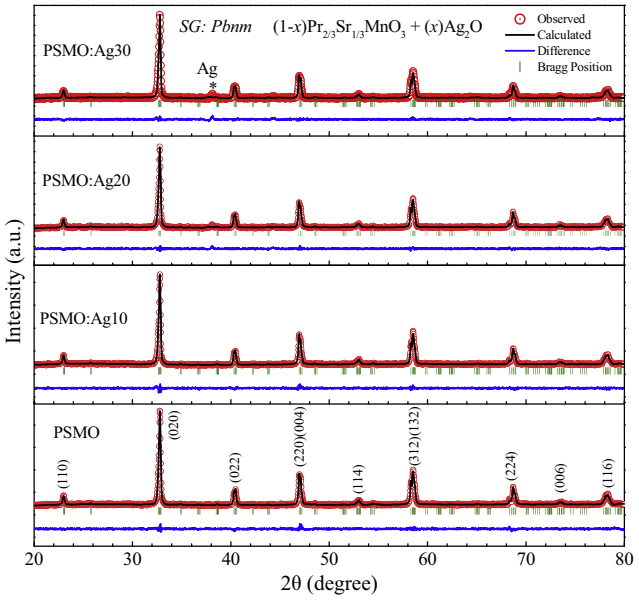

Fig. 1. Reitveld refined X-ray diffraction patterns for the composite series $(1-x)Pr_{2/3}Sr_{1/3}MnO_3 + (x)Ag_2O$.

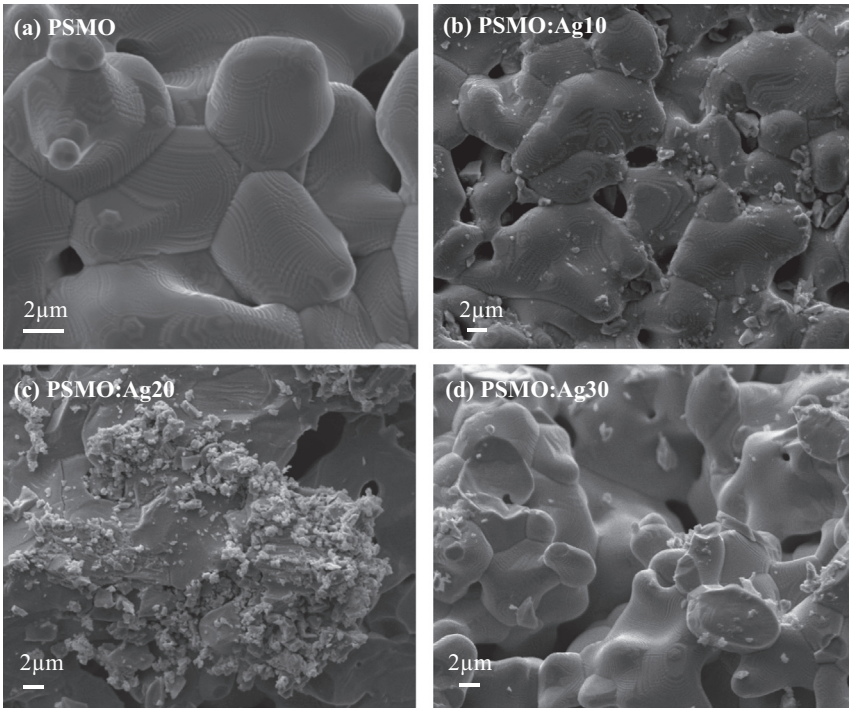

Fig. 2. Scanning electron micrographs of (a) PSMO, (b) PSMO:Ag10, (c) PSMO:Ag20 and (d) PSMO:Ag30 samples.

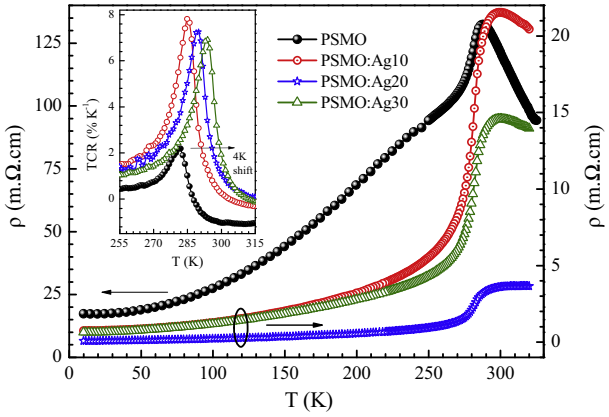

Fig. 3. Temperature dependence of the zero field electrical resistivity for pristine and 10%, 20% and 30% Ag_2O added PSMO samples. Inset shows the corresponding TCR of the samples with 4 K successive shift in temperature-axis.

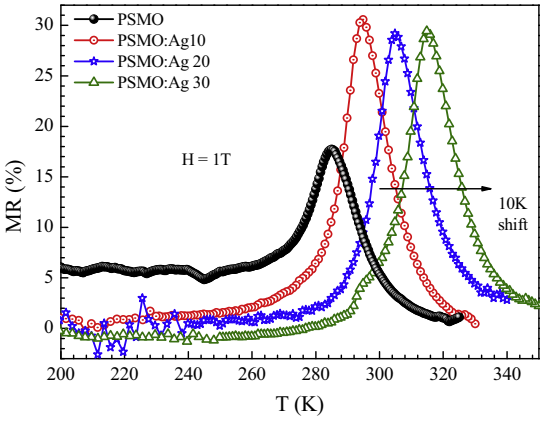

Fig. 4. Variation of magneto-resistance percentage with temperature at applied field of 1 T for pristine and 10%, 20% and 30% Ag_2O added PSMO samples with successive shift of 10 K in temperature-axis for resolving the overlapping peaks.

1.2 T in $La_{5/6}Ag_{1/6}MnO_3$ [16], 42% MR at 0.6 T (194 K) in $(Pr_{2/3}Ba_{1/3}MnO_3)_{0.73}Pd_{0.27}$ [17], 40%, 82% MR at 0.6 T, 5 T respectively (194 K) in $(Pr_{2/3}Ba_{1/3}MnO_3)_{0.7}Ag_{0.3}$ composite [18,19] and 33.5% MR at 1 T (284 K) with 9.7% K^{-1} TCR (281 K) in $Pr_{2/3}Sr_{1/3}MnO_3$:Pd30 composite [20]. The comparison clearly shows PSMO:Ag composite system as potential bolometric and magnetic sensing material.

The temperature dependence of the DC magnetization $M(T)$ for the composite series has been measured at a small applied field of 500 gauss in field cooled mode and is shown in Fig. 5. The 10 K shift towards the positive x-axis in the magnetization data is purposefully made to avoid the overlapping of the peaks. T_C of the samples are shown in the inset of Fig. 5, and are found close to 282 K. The nearly invariant T_C again confirms the fact that Ag does not occupy any lattice sites (i.e. Pr/Sr-site or the Mn-site) so that the Mn^{3+}–Mn^{4+} ratios remains unchanged. We can see that the overall moment (emu/g) has decreased for the Ag composites. This is due to the magnetic dilution effect of paramagnetic silver [13,15].

Fig. 6 shows isothermal magnetization $M(H)$ curves registered in magnetic field up to 3 T in a temperature range 276–310 K for (a) 10%, (b) 20% and (c) 30% Ag_2O added PSMO composites. In the FM region the isotherms are non-linear and above T_C in the PM region the isotherms become linear. To understand the order of transition, their Arrott plots M^2 versus (H/M) have been drawn using the magnetization isotherm data and are shown in Fig. 6(d)–(f) [21]. The nature of magnetic phase transition by Arrott plots can be understood using the Banerjee criterion [22]. According to this criterion, the positive slope of all the Arrott plots gives second order magnetic phase transition while negative slope of some of these plots suggest first order transition. In our case, absence of negative slope in all the Arrott plots of Ag-composites confirms the second order transition. According to the mean field theory for ferromagnetic long range order, the Arrott plot should show a set of parallel lines around T_C and at T_C and a straight line should pass through the origin [23–25]. In our case the Arrott plots

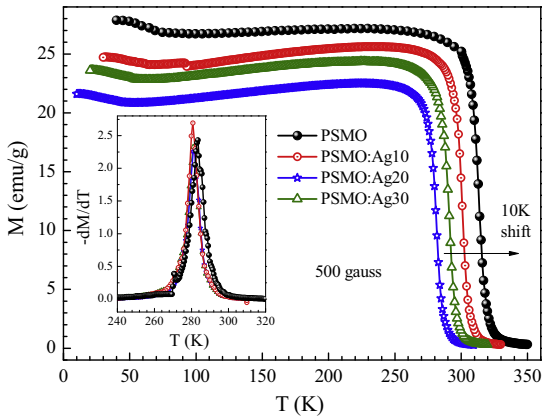

Fig. 5. Temperature dependent DC magnetization curve for the pristine and 10%, 20% and 30% Ag_2O added PSMO samples. Inset shows the corresponding $-dM/dT$.

do not follow the mean field theory and the lack of linearity in the Arrott plots suggest the existence of ferromagnetic short range order.

Assuming classical thermodynamics theory and using Maxwell's entropy relation, the expression for magnetic entropy change comes to be [26]:

$$\Delta S_M(T,H) = \int_0^{H_{max}} \left(\frac{\partial M(T,H)}{\partial T}\right)_H dH$$

In case of magnetization measurements performed at small discrete field and temperature intervals, this integral can be approximated as [27]:

$$|\Delta S_M| = \sum_i \frac{M_i - M_{i+1}}{T_{i+1} - T_i} \Delta H_i$$

where M_i and M_{i+1} are the experimental values of the magnetization at T_i and T_{i+1} respectively. The magnetic entropy change (ΔS_M) for

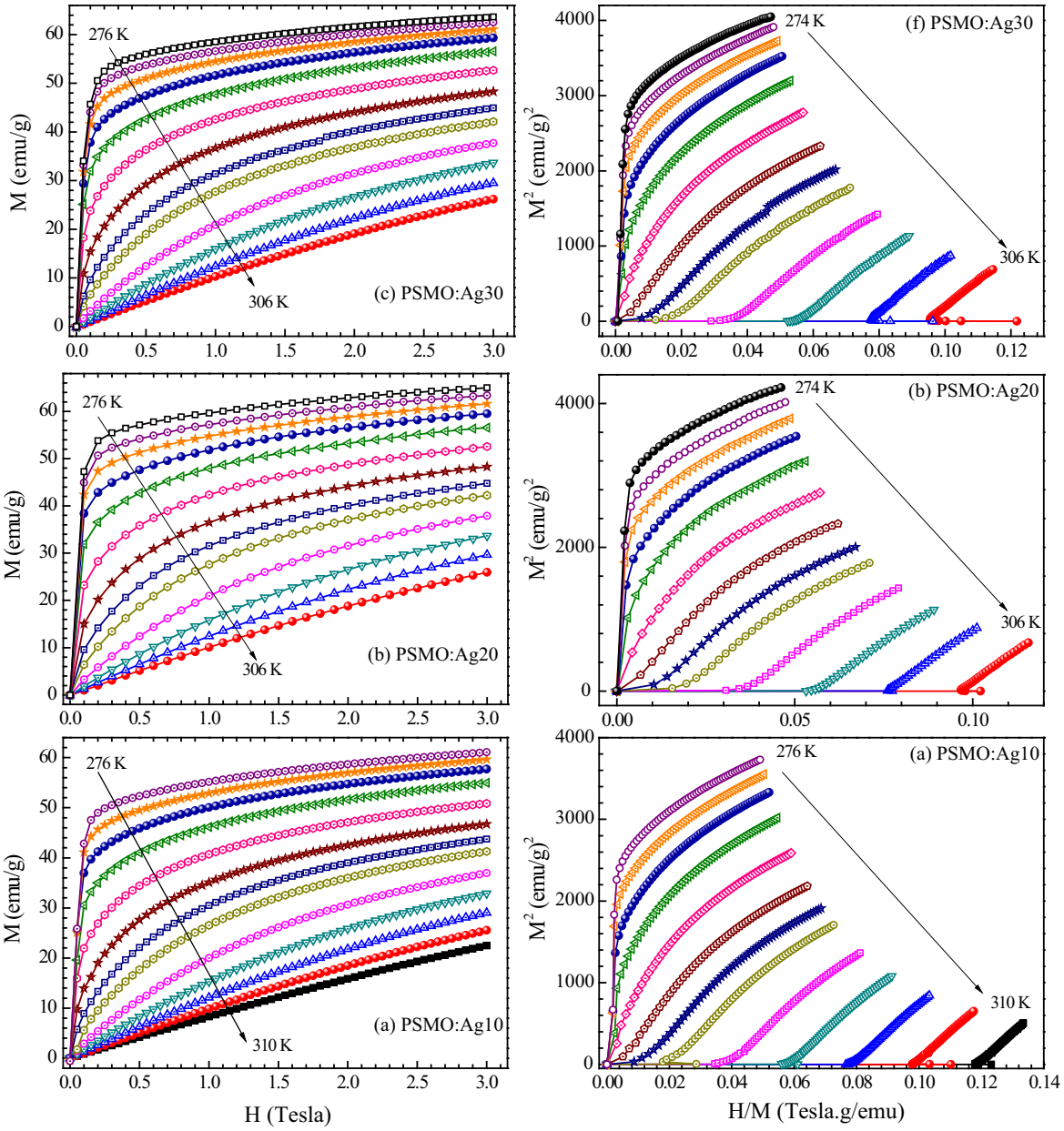

Fig. 6. (a)–(c) Isothermal magnetization $M(H)$ curves at different temperatures for 10%, 20% and 30% Ag_2O added PSMO samples and (d)–(f) their corresponding M^2–(H/M) Arrott plots.

PSMO:Ag composites has been calculated using the isothermal magnetization data. Fig. 7 shows the temperature dependence of magnetic entropy change (ΔS_M) for PSMO, PSMO:Ag10, PSMO:Ag20 and PSMO:Ag30 samples at field variation of 0–3 T. The ΔS_M values have been found to be (i) 3.3 J kg^{-1} K^{-1} at 1 T, 5.8 J kg^{-1} K^{-1} at 2 T and 8 J kg^{-1} K^{-1} at 3 T for PSMO:Ag10, (ii) 3.3 J kg^{-1} K^{-1} at 1 T, 5.9 J kg^{-1} K^{-1} at 2 T and 8.1 J kg^{-1} K^{-1} at 3 T for PSMO:Ag20, and (iii) 3.5 J kg^{-1} K^{-1} at 1 T, 6.1 J kg^{-1} K^{-1} at 2 T and 8.4 J kg^{-1} K^{-1} at 3 T for PSMO:Ag30 composites respectively (Table 2). As may be seen from Fig. 7, these values for the composite are quite high in comparison to the pristine PSMO. The magnetic entropy change values show an increasing trend with increase in Ag concentration. From Fig. 7 it is evident that PSMO shows double peak nature (two transitions) at higher field value which is absent in the Ag composites. Since these samples were prepared in air so the pristine sample may possess oxygen content less than '3' in the grain boundary region. At lower applied magnetic field, all the grains/domains (oxygen rich/deficient) will try to rotate in the field direction. Therefore we will observe only single transition at lower field (Fig. 5). On the other hand, at high field values it seems that the oxygen less domains grow at a faster rate as compared to oxygen rich domains whose effect is clearly visible in the form of inhomogeneity or two transitions in Fig. 7. This feature is absent in composites since oxygen liberated from the dissociation of Ag–O bond replenishes the oxygen loss resulting in one type of domains and hence single transition at higher field also.

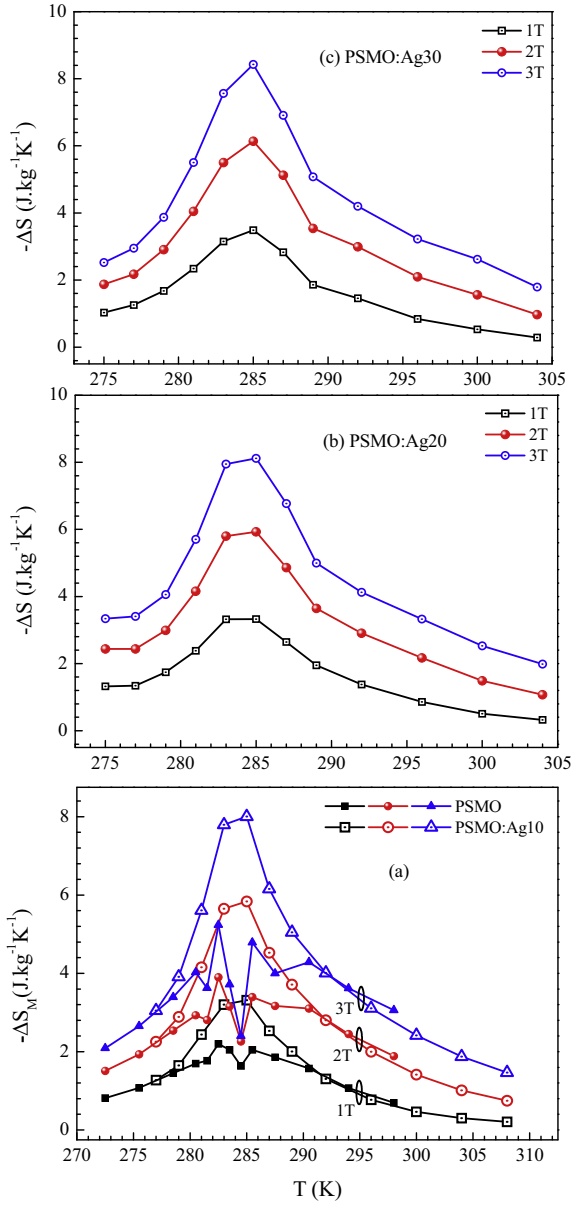

Fig. 7. Temperature dependence of magnetic entropy change (ΔS_M) for (a) PSMO and PSMO:Ag10, (b) PSMO:Ag20 and (c) PSMO:Ag30 samples at H = 1 T, 2 T and 3 T fields respectively.

Table 2
Experimental values of magnetic entropy change (ΔS_M) and refrigeration capacity for PSMO:Ag composites.

Samples	$\lvert\Delta S_M\rvert$ (J kg^{-1} K^{-1}) at			RC (J kg^{-1}) at		
	1 T	2 T	3 T	1 T	2 T	3 T
PSMO:Ag10	3.3	5.8	8	38.1	73.3	104.0
PSMO:Ag20	3.3	5.9	8.1	39.5	91.0	107.7
PSMO:Ag30	3.5	6.1	8.4	37.1	75.3	105.4

The magnetic cooling efficiency of a magnetocaloric material is defined as relative cooling power (RCP) or refrigeration capacity (RC) is calculated by taking the product of the peak ΔS_M value and the full-width at half maximum ($\delta T_{FWHM} = T_2 - T_1$) in the temperature dependent magnetic entropy change curve ($\Delta S_M - T$) as

$$RC = \Delta S_M \times \delta T_{FWHM}$$

Thus obtained RC values are found to be (i) 38.1 J kg^{-1} at 1 T, 73.3 J kg^{-1} at 2 T, 104.0 J kg^{-1} at 3 T for PSMO:Ag10, (ii) 39.5 J kg^{-1} at 1 T, 91.0 J kg^{-1} at 2 T, 107.7 J kg^{-1} at 3 T for PSMO:Ag20 and (iii) 37.1 J kg^{-1} at 1 T, 75.3 J kg^{-1} at 2 T, 105.4 J kg^{-1} at 3 T for PSMO:Ag30 composite respectively. The RC has been found to be maximum for PSMO:Ag20 and then decreased only marginally for PSMO:Ag30 composite (Table 2). The observed results on MCE in our case have been found to be comparable or greater than some of reported values in literature viz. ΔS_M of 8.52 J kg^{-1} K^{-1} at 5 T (300 K) in $Pr_{0.63}Sr_{0.37}MnO_3$ single crystal [3], ΔS_M of 7.6 J kg^{-1} K^{-1} at 5 T (298 K) in $La_{0.7}Ca_{0.2}Sr_{0.1}$:Ag10 [5], ΔS_M of 3.5 J kg^{-1} K^{-1} at 1 T, 6.3 J kg^{-1} K^{-1} at 2 T, 8.7 J kg^{-1} K^{-1} at 3 T and RC of 34.7 J kg^{-1} at 1 T, 65.5 J kg^{-1} at 2 T, 87.9 J kg^{-1} at 3 T (283 K) in $Pr_{2/3}Sr_{1/3}MnO_3$:Pd10 composite (our earlier work) [20], ΔS_M of (2.6–3.3) J kg^{-1} K^{-1} and RC of (57–98) J kg^{-1} at 2.6 T (287–303 K) in La-deficient $La_{0.8}Ag_{0.1}MnO_3$ system [28], ΔS_M of 2.8 to 5.6 J kg^{-1} K^{-1} and RC of 68 to 118 J kg^{-1} at 2.6 T (269–303 K) in (L-Ag)MnO_3 system [29], ΔS_M of 2.3 J kg^{-1} K^{-1} and RC of 34.5 J kg^{-1} at 2.5 T (320 K) in $Pr_{0.6}Sr_{0.4}MnO_3$ [30], ΔS_M of 1.84 J kg^{-1} K^{-1} and RC of 92 J kg^{-1} at 2 T (300 K) in $Pr_{0.6}Sr_{0.35}Na_{0.05}MnO_3$ [31], ΔS_M of 4.81 J kg^{-1} K^{-1} and RC of 260.7 J kg^{-1} at 5 T (160 K) in Sr deficient $Pr_{0.6}Sr_{0.35}MnO_3$ [32], ΔS_M of 3.8 J kg^{-1} K^{-1} and RC of 295 J kg^{-1} at 5 T (275 K) in $Pr_{0.52}Sr_{0.48}MnO_3$ single crystal [33]. Thus the studied PSMO:Ag composite series having high 7.8% K^{-1} TCR, 30.5% MR at 1 T and large magnetocaloric effect (ΔS_M of 3.5 J kg^{-1} K^{-1} at 1 T, 6.1 J kg^{-1} K^{-1} at 2 T and 8.4 J kg^{-1} K^{-1} at 3 T and RC of 39.5 J kg^{-1} at 1 T, 91.0 J kg^{-1} at 2 T, 107.7 J kg^{-1} at 3 T) makes the studied composite system a potential candidate for the bolometric, magnetic sensing and magnetic refrigerating based devices near room temperature.

4. Conclusions

Magneto-transport and magnetocaloric effect in $Pr_{2/3}Sr_{1/3}MnO_3$:Ag_2O (PSMO:Ag) with Ag_2O (10–30 mol%) have been studied by resistivity and magnetization measurements. Temperature coefficient of resistance (TCR), magneto-resistance (MR) and magnetocaloric properties of the composite have shown different responses to the Ag addition. TCR changes randomly with Ag, first increases for PSMO:Ag10 composite to 7.8% K^{-1} and then decreases marginally

with increasing Ag content. MR has been found to show a maximum value of 30.5% at 1 T applied field for PSMO:Ag10 composite. Magnetic entropy change (ΔS_M) increased with increasing Ag content and found to be 3.5 J kg^{-1} K^{-1} (1 T), 6.1 J kg^{-1} K^{-1} (2 T) and 8.4 J kg^{-1} K^{-1} (3 T) for PSMO:Ag30 composite at 285 K. The maximum refrigeration capacity (RC) has been found to be 39.5 J kg^{-1} (1 T), 91.0 J kg^{-1} (2 T) and 107.7 J kg^{-1} (3 T) for the PSMO:Ag20 composite. TCR, MR, ΔS_M, and RC values have been compared with some existing reports in literature and have been found to perform better. PSMO:Ag composite, therefore exhibits potential for bolometric, magnetic sensing and magnetic refrigerating applications near room temperature.

Acknowledgements

Authors thank the Director, National Physical Laboratory (CSIR), India, for his support and encouragement. Scientific interactions with Dr. Neeraj Panwar of the Central University of Rajasthan are also gratefully acknowledged. The authors (RCB and HK) would like to acknowledge the financial assistance from the CSIR, India under the Emeritus Scientist Scheme.

References

[1] M.-H. Phan, S.-C. Yu, J. Magn. Magn. Mater. 308 (2007) 325.
[2] B.F. Yu, Q. Gao, B. Zhang, X.Z. Meng, Z. Chen, Int. J. Refrig. 26 (2003) 622.
[3] M.-H. Phan, H.-X. Peng, S.-C. Yu, J. Appl. Phys. 97 (2005) 10M306.
[4] V.P.S. Awana, R. Tripathi, N. Kumar, H. Kishan, G.L. Bhalla, R. Zeng, L.S. Chandra, V. Ganesan, H.-U. Habermeier, J. Appl. Phys. 107 (2010) 09D723.
[5] R. Jha, S.K. Singh, A. Kumar, V.P. Awana, J. Magn. Magn. Mater. 324 (2012) 2849.
[6] R. Tripathi, V.P.S. Awana, N. Panwar, G.L. Bhalla, H.U. Habermier, S.K. Agarwal, H. Kishan, J. Phys. D. Appl. Phys. 42 (2009) 175002.
[7] V.P.S. Awana, R. Tripathi, S. Balamurugan, H. Kishan, E. Takayama-Muromachi, Solid State Commun. 140 (2006) 410.
[8] Q. Xu, R. Wang, Z. Zhang, Phys. Rev. B 71 (2005) 092401.
[9] R.D. Shannon, Acta Crystallogr. Sect. A 32 (1976) 751.
[10] X.-B. Yuan, Y.-H. Liu, C.-J. Wang, L.-M. Mei, J. Phys. D. Appl. Phys. 38 (2005) 3360.
[11] T. Tang, Q.Q. Cao, K.M. Gu, H.Y. Xu, S.Y. Zhang, Y.W. Du, Appl. Phys. Lett. 77 (2000) 723.
[12] R.C. Bhatt, P.C. Srivastava, S.K. Agarwal, V.P.S. Awana, J. Supercond. Nov. Magn. 27 (2014) 1491.
[13] Y.-H. Huang, C.-H. Yan, F. Luo, W. Song, Z.-M. Wang, C.-S. Liao, Appl. Phys. Lett. 81 (2002) 76.
[14] T. Tang, S.Y. Zhang, R.S. Huang, Y.W. Du, J. Alloys Comp. 353 (2003) 91.
[15] C.S. Xiong, L.G. Wei, Y.H. Xiong, J. Zhang, D.G. Li, Q.P. Huang, Y.D. Zhu, X.S. Li, J. Phys. D. Appl. Phys. 40 (2007) 1331.
[16] L. Pi, M. Hervieu, A. Maignan, C. Martin, B. Raveau, Solid State Commun. 126 (2003) 229.
[17] N. Panwar, I. Coondoo, S.K. Agarwal, Mater. Lett. 64 (2010) 2638.
[18] N. Panwar, D.K. Pandya, S.K. Agarwal, J. Phys. D. Appl. Phys. 40 (2007) 7548.
[19] N. Panwar, I. Coondoo, R.S. Singh, S.K. Agarwal, J. Alloys Comp. 507 (2010) 439.
[20] R.C. Bhatt, P.C. Srivastava, V.P.S. Awana, H. Kishan, S.K. Agarwal, Mater. Res. Express 1 (2014) 036107.
[21] A. Arrott, Phys. Rev. 108 (1957) 1394.
[22] B.K. Banerjee, Phys. Lett. 12 (1964) 16.
[23] H.E. Stanley, Introduction to Phase Transitions and Critical Phenomena, Oxford University Press, 1971.
[24] J. Mira, J. Rivas, F. Rivadulla, C. Vázquez-Vázquez, M.A. López-Quintela, Phys. Rev. B 60 (1999) 2998.
[25] L.E. Hueso, P. Sande, D.R. Miguens, J. Rivas, F. Rivadulla, M.A. Lopez-Quintela, J. Appl. Phys. 91 (2002) 9943.
[26] A.H. Morrish, The Physical Principles of Magnetism, Wiley, 2001.
[27] R.D. McMichael, J.J. Ritter, R.D. Shull, J. Appl. Phys. 73 (1993) 6946.
[28] A.G. Gamzatov, A.B. Batdalov, I.K. Kamilov, A.R. Kaul, N.A. Babushkina, Appl. Phys. Lett. 102 (2013) 032404.
[29] I.K. Kamilov, A.G. Gamzatov, A.M. Aliev, A.B. Batdalov, A.A. Aliverdiev, S.B. Abdulvagidov, O.V. Melnikov, O.Y. Gorbenko, A.R. Kaul, J. Phys. D. Appl. Phys. 40 (2007) 4413.
[30] S. Zemni, M. Baazaoui, J. Dhahri, H. Vincent, M. Oumezzine, Mater. Lett. 63 (2009) 489.
[31] R. Thaljaoui, W. Boujelben, M. Pękała, K. Pękała, J. Mucha, A. Cheikhrouhou, J. Alloys Comp. 558 (2013) 236.
[32] W.C. Koubaa, M. Koubaa, A. Cheikhrouhou, J. Alloys Comp. 509 (2011) 4363.
[33] M. Patra, S. Majumdar, S. Giri, G.N. Iles, T. Chatterji, J. Appl. Phys. 107 (2010) 076101.